Geotech Geol Eng (2018) 36:2343–2350
https://doi.org/10.1007/s10706-018-0466-2

ORIGINAL PAPER

Study on Micro-expansive Concrete-Filled Steel Tube Support for Controlling the Stability of Surrounding Rock in Deep Roadway

Limin Liu · Jinpeng Zhang

Received: 7 November 2017 / Accepted: 19 January 2018 / Published online: 25 January 2018

Abstract The overall supporting capacity of ordinary concrete-filled steel tube support (CFSTS) can be decreased due to the self-shrinkage of concrete and the cracks of hardened concrete. The micro-expansive CFSTS is put forward in this paper. Firstly, the optimum proportion of micro-expansion concrete was determined by concrete strength testing. Then, the deformation of micro-expansion CFSTS and ordinary CFSTS under the same load w studied by numerical simulation. Finally, the micro-expansion CFSTS and ordinary CFSTS were applied to the roadway respectively. The results show: The expansive agent content and water reducer content is 11 and 0.5% in the optimum proportion of micro-expansive concrete, respectively. Under the same load, the deformation of the ordinary CFSTS was much larger than that of the micro-expansion CFSTS. The deformations of roof–floor and two sides of roadway supported by the micro-expansion CFSTS were obviously smaller than that of roadway supported by the ordinary CFSTS. The micro-expansion CFSTS has stronger supporting capacity than ordinary CFSTS.

Keywords Micro-expansion CFSTS · Ordinary CFSTS · Optimum proportion · Supporting capacity

L. Liu · J. Zhang (✉)
College of Mining and Safety Engineering, Shandong University of Science and Technology, Qingdao 266590, Shandong, China
e-mail: zhljinpeng@163.com; lmliuhhu@163.com

1 Introduction

Concrete-filled steel tube has been widely used in engineering. When the concrete is poured into the steel tube and reaches a certain strength, the concrete ensures the local stability of the thin-walled steel tube. In turn, the steel tube constrains the radial deformation of the concrete, which makes it in three direction stress state and delays the pressure longitudinal cracking, thereby enhancing the bearing capacity of concrete-filled steel tube (Wu et al. 2014; Wei et al. 2014; Mahgub et al. 2017). As a composite structure, CFST has the unique working characteristics: elastic working and plastic failure, high bearing capacity and large limit compression deformation (Chen et al. 2017a, b, c; Dong et al. 2017; Liu et al. 2017).

With the advantages of high bearing capacity, corrosion resistance, ease of construction and so on, CFST is widely used in civil engineering (Nie et al. 2014; Guo et al. 2012). In addition, some scholars study the composite structure of CFST and steel bar. Moon et al. (2013) studied on the variation of the strength of CFST with or without reinforcement under the mixed load. Fong et al. (2011) designed truss structure composed by steel tube filled with steel bar and concrete and studied its the mechanical properties.

According to the application of CFST in civil engineering, CFST is extended to the roadway support field. So, CFSTS is developed. CFSTS has been proposed as a new passive support form for controlling the stability of surrounding rock in underground

structures, especially for the case of high ground stress. CFSTS can provide higher supporting force than U-shaped steel supports and better control the deformation of surrounding rock mass. Gao et al. (2010), Wang (2009) and Gao et al. (2009) had put forward the CFSTS for controlling the stability of surrounding rock in underground structures and carried on experiments and applications. Xu et al. (2014a, b) presented a numerical study on the mechanical performance of CFSTS.

After the ordinary concrete is poured into the steel tube and hardened, the overall supporting capacity of CFSTS is decreased due to the self-shrinkage of concrete and the cracks of hardened concrete. So, only the concrete to enrich the steel tube, can the bearing capacity of CFSTS be fully played. To ensure the hardened concrete enriched the steel tube support, the micro-expansive CFSTS is put forward in this paper. Micro-expansion concrete can offset the self-shrinkage of concrete by volume expansion and improve the overall supporting capacity of CFSTS.

2 Proportioning Test of Micro-expansive Concrete

In order to ensure that the hardened concrete enriched the steel tube support to prevent the self-shrinkage of concrete and the cracks of hardened concrete, the expansive agent is added into the concrete. According to <Specification for Design of Mix Proportion of Ordinary Concrete>, the multi-group concrete proportion is designed. The optimum ratio of concrete is selected by the test analysis of the strength of concrete.

2.1 Raw Material Selection

1. Cement. The 42.5# ordinary portland cement is selected in this experiment.
2. Expansive agent. The calcium aluminate expansive agent is used and its content is between 10 and 12%.
3. Water reducer. The amount of water requirement to make up shrink-compensated concrete is relatively large. Increasing the amount of water requirement can increase the water–cement ratio, reduce the expansion rate and increase the dry shrinkage. Therefore, water reducer should be added. MF superplasticizer was selected.
4. Aggregate. According to "Building Gravel" (GB/T14685-2001), the high quality river sand was selected as fine aggregate and the crushed stone with particle size of 5–10 mm was chosen as coarse aggregate.

2.2 Preliminary Calculation of Mixing Ratio

The uniaxial compressive strength of compensating shrinkage concrete for 28 days needs to be 40 MPa. According to the performance of raw materials and technical requirement of concrete, calculate the general scope of raw materials. Then, the optimum proportion of concrete for meeting the requirements of workability and strength is determined by the laboratory test.

1. Concrete strength

According to the rules of JGJ55-2000, the strength of concrete is as follow:

$$f_{cu,0} = f_{cu,k} + t \cdot \sigma \tag{1}$$

where $f_{cu,0}$ represents the strength of concrete (MPa); $f_{cu,k}$ represents strength grade of concrete (MPa); t represents the σ guarantee rate of strength, generally take 1.645; represents the standard deviation of concrete strength (MPa), when the strength of concrete is greater than C35, $\sigma = 6.0$.

Therefore,

$$f_{cu,0} = 40 + 1.645 \times 6.0 = 49.87\,\text{MPa}$$

2. Water–cement ratio of concrete

According to the formula:

$$\frac{W}{C} = \frac{Af_{ce}}{f_{cu,0} + ABf_{ce}} \tag{2}$$

where W represents the amount of water per cubic concrete (kg); C represents the amount of cement per cubic concrete (kg); $f_{ce} = 1.13f_c$, f_c is the strength grade of cement; A and B represent the empirical coefficients, A = 0.46, B = 0.07.

Therefore, water–cement ratio is as follow:

$$\frac{W}{C} = \frac{0.46 \times 1.13 \times 40}{49.87 + 0.46 \times 0.07 \times 1.13 \times 40} = 0.405$$

3. The amount of cement and water

The amount of cement is no less than 300 kg/m^3. According to the empirical formula, the amount of cement takes 350 kg/m^3, so the amount of water W = 0.405 × 350 = 141.75 kg/m^3. According to the principle of unified slump, the amount of water reduced after using water reducer.

4. The content of coarse and fine aggregate (S_0, G_0)

It is assumed that the volume of the concrete mixture is equal to the sum of the volume of each constituent material and the volume of air contained in the mixture. The content of each material in concrete of 1 m^3 can be calculated by formula (3). The sand rate can be calculated by formula (4). The content of sand and stone in concrete of 1 m^3 can be calculated by formula (3) and (4).

$$\frac{C_0}{\rho_0}+\frac{S_0}{\rho_{0S}}+\frac{G_0}{\rho_{0g}}+\frac{W_0}{\rho_w}+10\alpha=1000L \tag{3}$$

$$S_P=\frac{S_0}{S_0+G_0}\times 100\% \tag{4}$$

where C_0 and W_0 represent the amount of cement and water in 1 m^3 concrete (kg); S_0 and G_0 represent the content of sand and gravel, kg; ρ_c and ρ_w represent the density of cement and water (g/cm^3), usually $\rho_c = 3.1$, $\rho_w = 1.0$; ρ_{0s} and ρ_0 represent the density of sand and stone in concrete (g/cm^3), the sand density is 1.47 g/cm^3, the stone density is 1.45 g/cm^3; α represents the percentage of gas in concrete, when the gas forming admixture is not used, $\alpha = 1$; S_p represents the ratio of sand in concrete (%).

Take $S_p = 33\%$, calculated by simultaneous Eqs. (3) and (4): $S_0 = 353.5$ kg, $G_0 = 707.7$ kg.

2.3 Strength Test of Concrete

The expansive agent is added in the form of replacing cement. The water reducer is added in the form of additional addition. According to the apparent characteristics of concrete, the content of sand, stone and so on should be adjusted. CSS44100 electronic universal testing machine is Fig. 1.

Through the above calculation, the proportion of cement, sand and stone is 1:1.31:2.65. According to the different content of water reducer, three groups of experimental scheme were designed. The content of water reducer in the experiment were 0.3, 0.5 and 0.7%, respectively. In each group of experiments, the content of expansive agent was 10 and 11%, respectively. Under the premise of ensuring workability and slump of concrete, the standard concrete block was made. The compressive strength of the specimens was measured every 4 days until the 28 day. The compressive strength of the stone body at 4, 8, 12, 16, 20, 24 and 28 days were measured by employing a 300-kN CSS44100 electronic universal testing machine, respectively. The test results are shown in Fig. 2.

Figure 2 shows that: in the first group of tests, the compressive strengths of the concrete specimens with expansive agent content of 10 and 11% are 49.3 and 52.6 MPa, respectively. In the second group of tests, the compressive strengths of the concrete specimens with expansive agent content of 10 and 11% are 52.5 and 55.4 MPa, respectively. In the third group of tests, the compressive strengths of the concrete specimens with expansive agent content of 10 and 11% are 50.8 and 52.6 MPa, respectively.

Under the same content of water reducer, the compressive strength of the concrete specimens increases when the content of expansive agent increases from 10 to 11%. The comparative analysis of the three groups of tests shows that under the same content of expansive agent, the compressive strength

Fig. 1 CSS44100 electronic universal testing machine

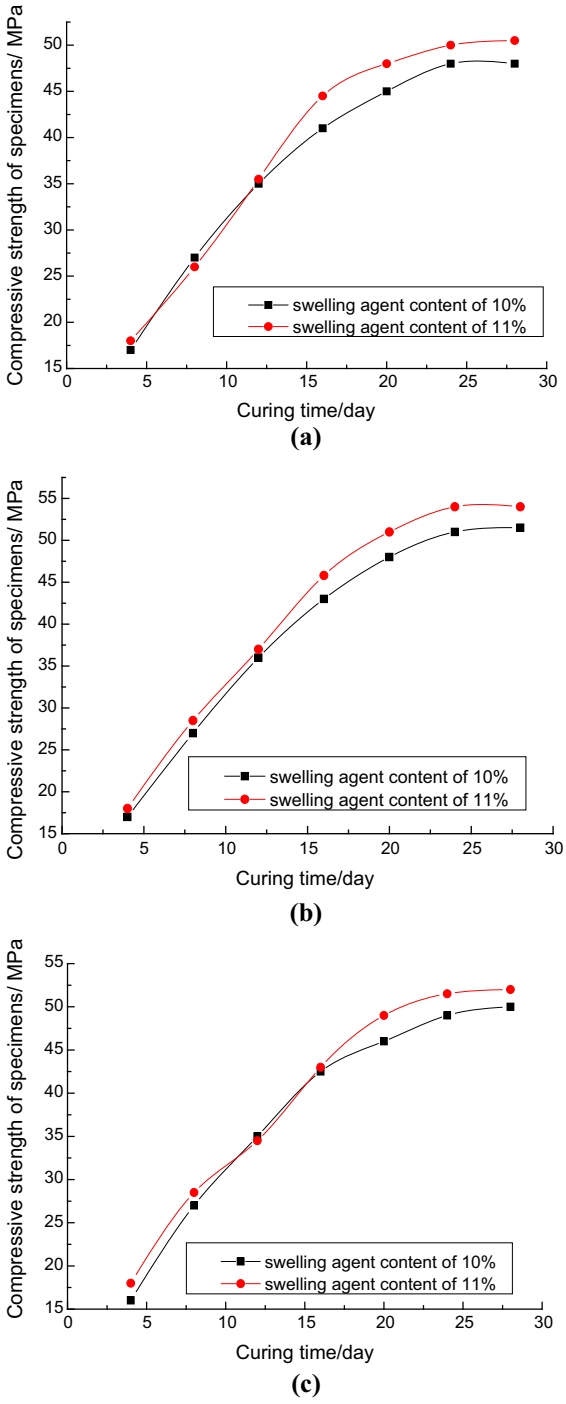

Fig. 2 The compressive strength of concrete specimens varies with time. **a** Water reducer content of 0.3%, **b** water reducer content of 0.5%, **c** water reducer content of 0.7%

of the concrete specimens increases significantly when the content of the water reducer is increased from 0.3 to 0.5%. When the content of the water reducer is increased from 0.5 to 0.8%, the growth range of the compressive strength of the concrete specimens is small or decreased. Through comprehensive analysis of the compressive strength (test results in Fig. 2), slump, fluidity, workability and other relevant parameters of the concrete specimens, finally determined: the ratio of cement, sand, gravel = 1:1.31:2.65, water–cement ratio of 0.41, the content of expansive agent and water reducer is 11 and 0.5%, respectively.

3 Bearing Capacity of Micro-expansive Concrete Filled Steel Tube Support

The micro-expansion concrete with above optimum proportion and ordinary concrete filled the steel tube support, respectively. Then, set as scheme 1 (micro-expansion CFSTS) and scheme 2 (ordinary CFSTS). Under the same load, the deformations of the scheme 1 and scheme 2 were analyzed by numerical simulation. No expansive agent is added to the concrete in scheme 1 and 11% of expansive agent is added to the concrete in scheme 2, and the rest of the raw material are the same. The model is set to plane strain model and free grid division. The model is divided into quadrilateral element and simulated by plane 42 element. The material parameters of steel tube and concrete are shown in Tables 1 and 2.

The boundary conditions of CFSTS. The bottom of support is fixed and the top of that is subjected to stress analysis. Taking into account the impact of horizontal stress on the supports, applying pressure to the side arch is the same as the top pressure. According to the geological conditions, the estimated pressure is 15MP. So, the top and side arch of the CFSTS at the same time are added the surface force of 15MP. In order to facilitate the calculation of horseshoe-shaped support, the horseshoe-shaped support's structure is simplified as the following figure of the semi-circular arch supports. The simplified model is shown in Fig. 3. This model is mainly composed of the top arch section and two side arch sections of the horseshoe-shaped support. The three arch sections are the same and the corresponding center angle of each arch section is 70°. Then, the same load is applied to the top arch section and two side arch sections of the model, and the displacement constraints are applied to two ends of arch support.

Table 1 The steel tube unit material parameter

Material	Poisson ratio	Elastic modulus (N/mm^2)	Plastic modulus (N/mm^2)	Yield stress (N/mm^2)	Density (g/cm^3)
Q235 steel tube	0.280	2.06×10^5	0.15×10^5	300	7.85

Table 2 The concrete unit material parameter

Material	Poisson ratio	Elastic modulus (N/mm^2)	Cohesion (N/mm^2)	Friction angle	Expansion angle
C60 concrete	0.2	3.65 × 104	5.5654	55.6°	30°

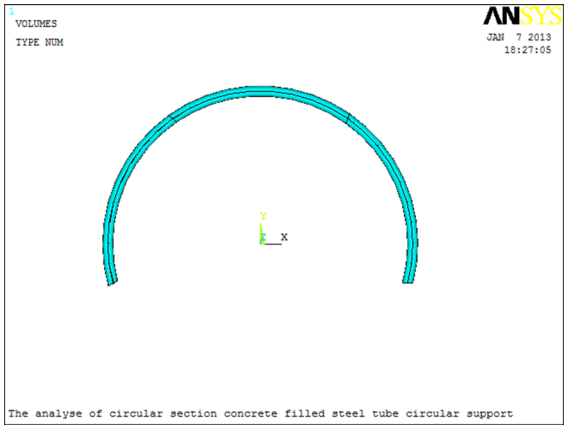

Fig. 3 Simplified model of CFSTS

The displacement of the micro-expansion CFSTS is shown in Fig. 4.

The displacement of the ordinary CFSTS is shown in Fig. 5.

The displacement diagram shows: when the uniform load is applied to the CFSTS, the displacement at the top of the CFSTS is the largest and the displacement at the bottom of it is close to 0. The displacement from the bottom to the top of the CFSTS is gradually increased. It shows that the simulation results are in accordance with the theory and the experimental data is of reference value.

As can be seen from the comparative analysis of Figs. 4 and 5, the displacement of the micro-expansion CFSTS is 0.004596 mm and the displacement of the ordinary CFSTS is 0.94863 mm. When the same load is applied to CFSTS, the deformation of the ordinary CFSTS is much larger than that of the micro-expansion CFSTS. The bearing capacity of the micro-expansion CFSTS is higher than that of the ordinary CFSTS.

4 Engineering Application

4.1 General Situation of Engineering

Pingdingshan ten mines is located in the hilly country of the Ruhe south and the Shahe north. The terrain of

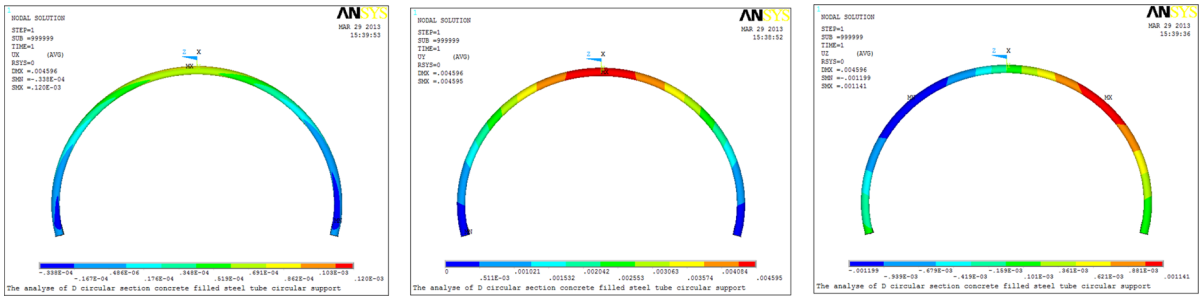

Fig. 4 Displacement diagram of X, Y and Z of micro-expansion CFSTS

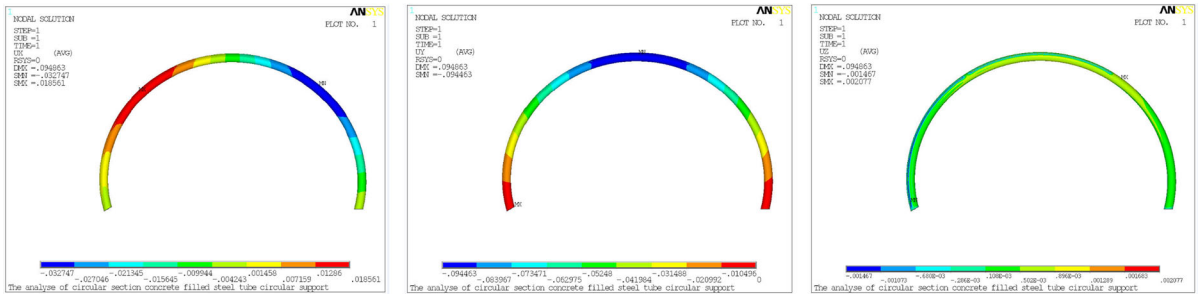

Fig. 5 Displacement diagram of X, Y and Z of ordinary CFSTS

mine field in the northwest is higher than that in the southeast. The strike length of the mine field from the east to west is 5.6 km and the inclination length of that from the north to the south is 7.0 km. The gross thickness of coal measures is about 900 m. The gross thickness of the main mineable coal is 13.74 m. The inclination angle of coal seam is 0–35°. Because of the occurrence condition of coal seam and the mountain in ground surface, the buried depth of coal seam is about 450–1100 m. The immediate roof and the immediate floor of coal seam are mainly sandy mudstone. The basic roof and the basic bottom of coal seam are mainly sandstone.

In order to compare and analyze the supporting effect of micro-expansion CFSTS and ordinary CFSTS in coal mine roadway, it is decided to set up two 100 m test roadways in Pingdingshan ten mines. The above-mentioned micro-expansion CFSTS and ordinary CFSTS are applied to the roadway respectively. According to the size and geological conditions of the roadway, design the size of steel support. According to the roadway size and geological conditions, the design of CFSTS size shown in Fig. 6. After the roadway was supported, the observation points were arranged in the roadway and multiple groups of observations were performed on the roof–floor of the roadway and two sides of roadway. Select the representative observations point to analyse. The roadway deformation evolution curve was shown in Fig. 7.

4.2 Structure Design of CFSTS

The CFSTS is designed as a horseshoe-shaped fully enclosed structure, which is composed of five steel tubes assembled through the sleeve. Figure 6 shows

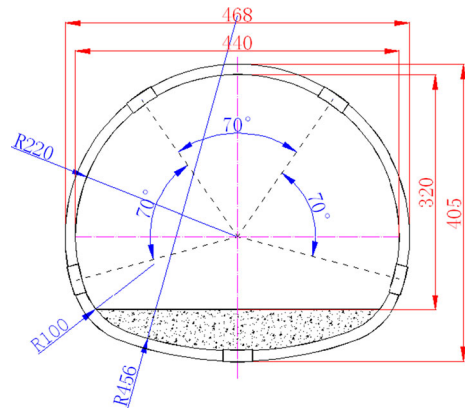

Fig. 6 Shape and size of the CFSTS

the shape and size of the CFSTS. The steel tube of Scenario 1 is filled with micro-expansion C60 concrete and the steel tube of Scenario 2 is filled with C60 ordinary concrete.

The components parameters of CFSTS: Select the steel tube (Q235 steel) of Φ150 × 5 mm. The circumference, width, height and spacing of the support are 11,530, 4680, 4050 and 650 mm, respectively. The size of the casing is Φ160 × 6.5 mm and the length of that is 400 mm.

4.3 Roadway Deformation Observation

Figure 7 is the deformation observation result of the representative observation points in the test roadway. As shown in Fig. 7, before 25 days, the deformation of roof–floor and the two sides of roadway gradually increase with the passage of time. After 25 days, the roadway deformation gradually tends to be stable. The final deformations of roof–floor and two sides of roadway supported by the micro-expansion CFSTS

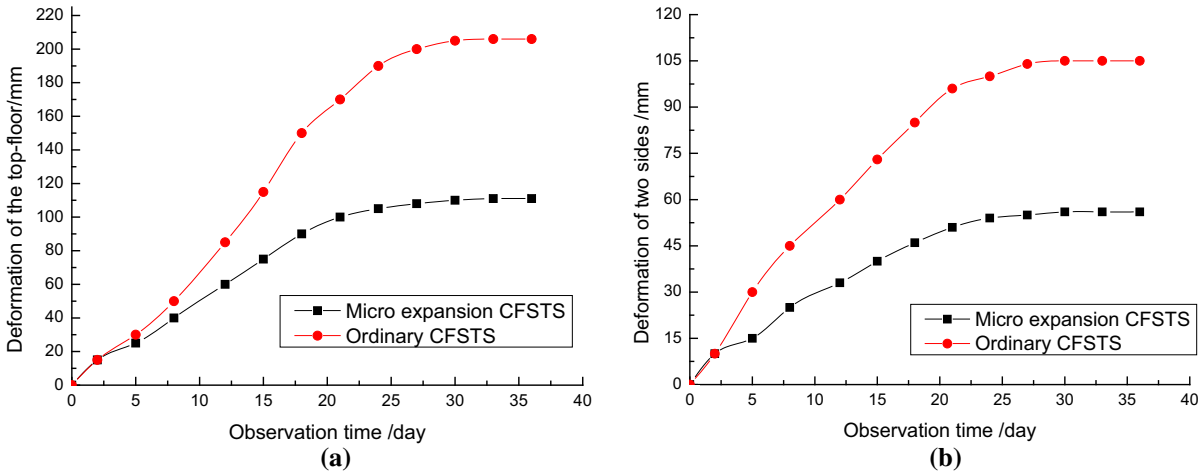

Fig. 7 Deformation observation result of the representative observation points in the test roadway. **a** Deformation of the roof–floor in test roadway, **b** deformation of the sides in test roadway

were 110 and 56 mm, respectively. The final deformations of roof–floor and two sides of roadway supported by the ordinary CFSTS were 205 and 105 mm, respectively. The final deformations of roof–floor and two sides of roadway supported by the micro-expansion CFSTS were obviously smaller than that of roadway supported by the ordinary CFSTS. It shows that the support effect of micro-expansion CFSTS is better than that of ordinary CFSTS, the micro-expansion CFSTS has stronger supporting capacity than ordinary CFSTS. In the working process of CFSTS, the concrete in micro-expansion CFSTS was always filled with steel tube. However, due to the self-shrinkage of concrete in ordinary CFSTS, the gap between concrete and steel tube occured, resulting in the deformation characteristics of the non-synchronous deformation of the concrete and steel tube, so that the bearing capacity of CFSTS significantly reduced.

5 Conclusion

1. Through the proportioning test of micro-expansive concrete, the optimum proportion was obtained: the ratio of cement, sand and gravel is l:1.31:2.65, water cement ratio is 0.41, the expansive agent content is 11%, water reducer content is 0.5%.
2. In the numerical model, the displacements of the micro-expansion CFSTS and the ordinary CFSTS are 0.004596 and 0.94863 mm, respectively. When the same load is applied to CFSTS, the deformation of the ordinary CFSTS is much larger than that of the micro-expansion CFSTS. The bearing capacity of the micro-expansion CFSTS is higher than that of the ordinary CFSTS.
3. The final deformations of roof–floor and two sides of roadway supported by the micro-expansion CFSTS were 110 and 56 mm, respectively. The final deformations of roof–floor and two sides of roadway supported by the ordinary CFSTS were 205 and 105 mm, respectively. It shows that the support effect of micro-expansion CFSTS is better than that of ordinary CFSTS, the micro-expansion CFSTS has stronger supporting capacity than ordinary CFSTS.

Acknowledgements The work described in this paper was fully supported by Graduate science and technology innovation project in Shandong University of Science and Technology (SDKDYC180204).

References

Chen J, Wang J, Jin WL (2017a) Concrete-filled steel tubes with reinforcing bars or angles under axial tension. J Constr Steel Res 133:374–382

Chen J, Wang J, Li W (2017b) Experimental behaviour of reinforced concrete-filled steel tubes under eccentric tension. J Constr Steel Res 136:91–100

Chen BC, Sheng Y, Famcd Amir et al (2017c) Torsional behavior of a new dumbbell-shaped concrete-filled steel tubes. Thin-Walled Struct 110:35–46

Dong CX, Kwan AKH, Ho JCM (2017) Effects of external confinement on structural performance of concrete-filled steel tubes. J Constr Steel Res 132:72–82

Fong M, Chan SL, Uy B (2011) Advanced design for trusses of steel and concrete-filled tubular sections. Eng Struct 33(12):3162–3171

Gao YF, Wang B, Qu GL et al (2009) Mechanical performance test of concrete filled steel tubular support and its application in roadway support. In: The eighth cross strait tunnel and underground engineering academic and technical seminar, China Taibei, vol 11, pp C15-1–C15-10 **(in Chinese)**

Gao YF, Wang B, Wang J et al (2010) Test on structural property and application of CFSTS of deep mine and soft rock roadway. Chin J Rock Mech Eng 29(1):2604–2609 **(in Chinese)**

Guo L, Li R, Fan F et al (2012) Study on hysteretic behaviors of composite frame–steel plate shear wall structures. China Civ Eng J 45(11):69–78

Liu LM, Zhang JP, Sun W et al (2017) Research and application of balance support design method for fully-mechanized gob-side entry driving with opposite mining direction. J Shandong Univ Sci Technol (Nat Sci) 36(6):24–31

Mahgub M, Ashour A, Lam D et al (2017) Tests of self-compacting concrete filled elliptical steel tube columns. Thin-Walled Struct 110:27–34

Moon J, Lehman DE, Roeder CW, Lee HE (2013) Strength of circular concrete-filled tubes with and without internal reinforcement under combined loading. Struct Eng ASCE 139:04013012

Nie JG, Wang YH, Fan JS (2014) Study on seismic behavior of concrete filled steel tube columns under pure torsion and compression–torsion combined action. China Civ Eng J 47(1):47–58

Wang B (2009) Analysis on the laws of tunnel deformation in soft rock and the supporting technology of CFSTS. China University of Mining and Technology (Beijing), Beijing **(in Chinese)**

Wei X, Han LH, Tao Z (2014) Flexural behaviour of curved concrete filled steel tubular trusses. J Constr Steel Res 93:119–134

Wu L, Han LH, Chan TM (2014) Tensile behaviour of concrete-filled double-skin steel tubular members. J Constr Steel Res 99:35–46

Xu W, Han LH, Tao Z (2014a) Flexural behaviour of curved concrete filled steel tubular trusses. J Constr Steel Res 93:119–134

Xu C, Luo XL, Zhu CX et al (2014b) Analysis of circular concrete-filled steel tube (CFT) support in high ground stress conditions. Tunn Undergr Space Technol 43:41–48